Online-Journals.org

iJOE International Journal of Online and Biomedical Engineering

iJOE | eISSN: 2626-8493 | Vol. 20 No. 6 (2024) | OPEN ACCESS

https://doi.org/10.3991/ijoe.v20i06.47293

PAPER

The Effect of Twisted Wire Configuration on the Stability of External Fixator: A Biomechanical Study

Alaa A. Najim[1](✉), Sadiq J. Hamandi[1], Ahmed Alzubaidi[2]

[1]Department of Biomedical Engineering College of Engineering, Al-Nahrain University, Baghdad, Iraq

[2]Department of Orthopedics, College of Medicine Al-Nahrain University, Baghdad, Iraq

st.alaa.a.najm@ced.nahrainuniv.edu.iq

ABSTRACT

The Ilizarov fixator is a type of external fixator that is used to treat patients who have suffered injuries from accidents, bone shortening, or nonunion of the bone. The principle behind the Ilizarov fixator is that thin wires (called Kirschner wires) are used to support the bones and connect them to framed rings. Before being fastened to the rings, the wires are tensioned and drilled through the bones. This study suggests using a new parallel wires configuration at the same level on the same ring and two revised versions, which are divergent and convergent models, and compare them with standard wires, 60 angle wires model. All models were designed using SolidWorks, a computer-aided design (CAD) software, and then analyzed in four conditions (axial compression, medial bending, posterior bending, and torsion) with Finite Element Analysis (FEA) using Ansys Workbench 2020 R2. Mechanical testing was conducted to validate the FEA results, A simple model consisting of a single ring, two K-wires, and polylactic acid (PLA) cylinders was utilized in a tensile test. It has been concluded from the results that the parallel model and its improvement have higher stiffness to axial compression, medial bending, and torsion, but a lower posterior bending stiffness, except the divergent model with 8-hole separation which has a relatively acceptable stiffness for posterior bending.

KEYWORDS

Ilizarov fixation, external fixation, orthopedic fixation, stability, bone segment stability, computational modelling simulation

1 INTRODUCTION

Illizarov fixators are applied on patients having injuries during accidents, shortening of the bone and nonunion of the bone. The surgeons fix the Illizarov fixator on the patient's leg. Many configurations of the Illizarov fixators can be made, and it depends on the injury on the patient. The principle of the Ilizarov is that bones are supported to the framed rings by thin wires (Kirschner wires) that were tensioned before being fastened to the rings after drilling through the bones healing as shown

Najim, A.A., Hamandi, S.J., Alzubaidi, A. (2024). The Effect of Twisted Wire Configuration on the Stability of External Fixator: A Biomechanical Study. *International Journal of Online and Biomedical Engineering (iJOE)*, 20(6), pp. 167–181. https://doi.org/10.3991/ijoe.v20i06.47293

Article submitted 2023-12-10. Revision uploaded 2024-01-18. Final acceptance 2024-01-18.

in Figure 1. One of the critical characteristics of the Ilizarov fixator is patient movability early in the course of therapy, which influences the best possible bone regeneration through the functional activity of the limb's muscles and joints. Moreover, the weight-bearing causes very minor cyclical axial strain in the fracture space, promoting additional osteogenic processes [1,2].

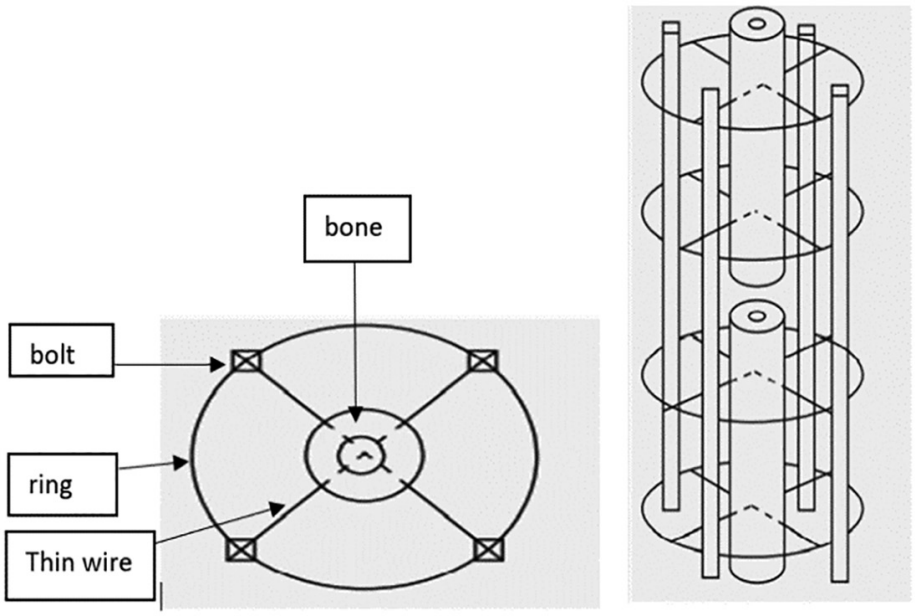

Fig. 1. Standard Ilizarov fixation

In order for the Ilizarov apparatus to function properly, wires must be tensioned precisely and securely fastened to the frame. The tensioning process is based on the fundamental biomechanical concept of axial mechanical stress and micro-movements in the osteogenic zone of the fracture area, which helps bridge the gap between the bones. The stiffness of the Ilizarov apparatus depends on the wire pretension used, and if this pretension is lost, the bone fragment's axial displacement will increase [3,4].

The Ilizarov fixator's stability is directly proportional to the wire's arrangement [5]. An unstable state arises when the crossing angle is less than 60 degrees, and this design significantly reduces stability in shear and bending, since in some cases, the surgeons cannot insert two transosseous wires in the bone at 90–60° angle and a single transosseous wire is insufficient [6]. This paper suggests using parallel transosseous wire fixation, as using a parallel wire will reduce the transfixation of a bulk of the muscles, which causes soreness and swelling that tie up patient mobilization, and the angle between the wires won't be a problem. Parallel wire fixation was suggested in 1995 but each wire is attached to a separate ring as shown in Figure 2, and it has been concluded that the basic form of parallel wires is not as rigid as the crossed wires in vertical bending and in shear loading. However, changing the wires in-between distance to 5 or 6 cm produces an equal bending rigidity [7,8].

However, this paper introduces a crucial modification to the standard wire utilized in Ilizarov fixation, which is the parallel transosseous wire and its modified models, that eliminates the need for crossing angle concerns. This paper aims to investigate the effectiveness of the modified models in resisting axial compression, medial and posterior bending, and torsion.

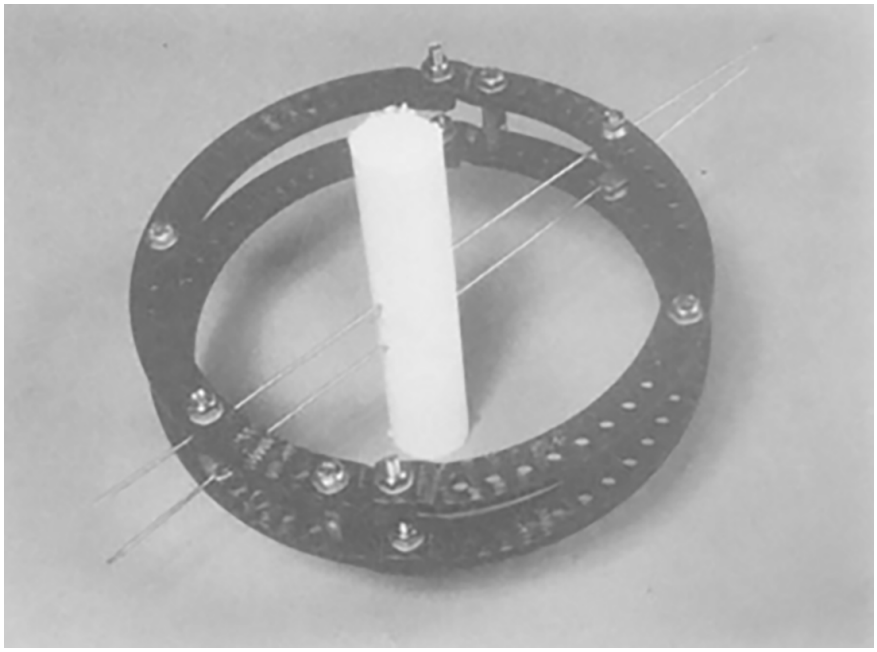

Fig. 2. The ring unit of the parallel wire suggested previously where each wire is attached to a separate ring [8]

2 MATERIALS AND METHODS

2.1 Experimental design

For testing different wire configurations, a model with a single carbon fiber ring with inner and outer diameters of 180mm and 210mm respectively and a depth of 4 mm having 46 holes each with 8 mm diameter, 2mm 316L stainless steel k-wires, stainless steel cannulated bolts, and 3cm diameter polylactic acid (PLA) cylinders of 10cm length were used to mimic the tibia as shown in Figure 3.

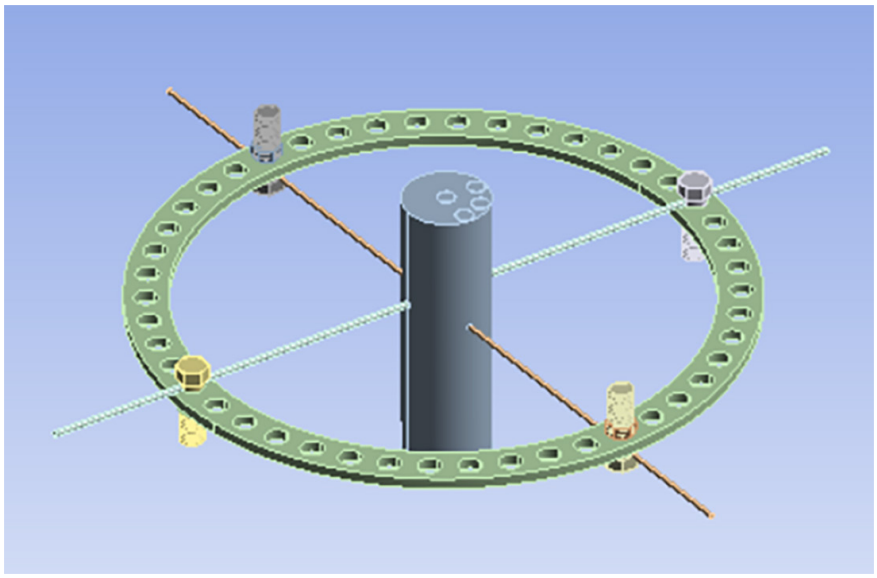

Fig. 3. The simple model used to test different wire configurations. In this case, the model is the standard wires

PLA materials are durable, easy to shape, and can be designed to mimic the mechanical properties of real bones to some extent [9,10]. The deformation and buckling of the ring were ensured not to affect the wires, so the model was firmly secured to a rigid iron support made up of six shafts, each with a 20mm diameter and 180mm length. These shafts have been securely welded to a base that measures 24 × 24cm of 10mm thickness as shown in Figure 4.

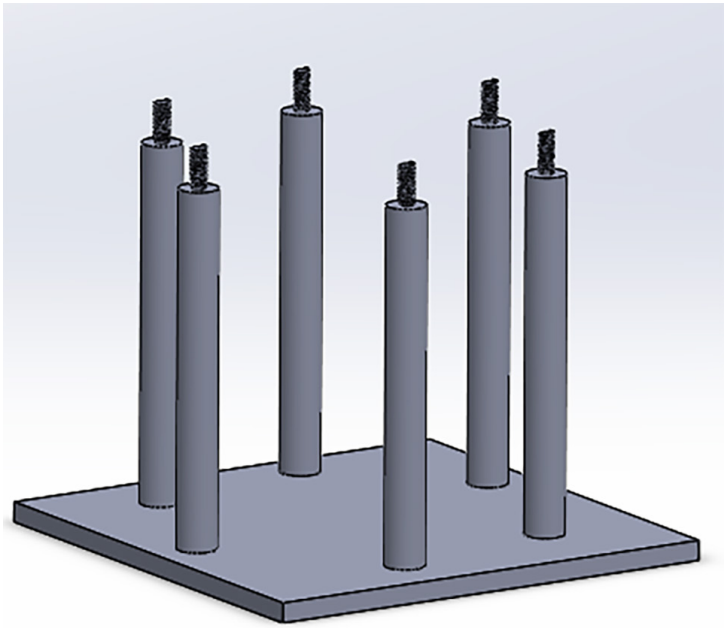

Fig. 4. Iron support frame

The first wire layout includes a 90-degree crossing angle above and below the ring with mediolateral and anteroposterior orientation, respectively, as illustrated in Figure 5a, which is the most stable and favored configuration. However, this is not feasible at some bone levels [11]. The second model was the same as the first, but with a 60-degree crossing angle wire, which is the second most favorable, and is illustrated in Figure 5b. The third model used a parallel design, with two wires placed above the ring as far apart as possible at the medio-lateral level. However, since the cylinder has a diameter of 3cm, the wires were placed at two adjacent holes in the ring as illustrated in Figure 5c. The fourth design consisted of one wire inserted above the ring at the medio-lateral level as shown in Figure 5d. Four modified designs of the parallel wire were used, including convergent and divergent wire configurations. The fifth model had a divergent 1-hole separation wire as illustrated in Figure 5e, the sixth model was convergent with 1-hole separation wire as illustrated in Figure 5f, the seventh had a divergent 8-hole separation wire as illustrated in Figure 5g, and the last was convergent with 8-hole separation wire as illustrated in Figure 5h.

2.2 Tensile test

The PLA cylinders were predrilled of 2mm hole for the wire insertion, then the wires attached to the ring by cannulated bolts with tightening one side of the wire by bolt and leaving the other side bolt untightened so the wires can be tensioned using

(computer controlled electronic universal testing machine of max load 50kN) to a 90 kg (883 N) to increase it stiffness, as shown in Figure 6, after the wire tensioned the bolt, tightened and removed from the machine.

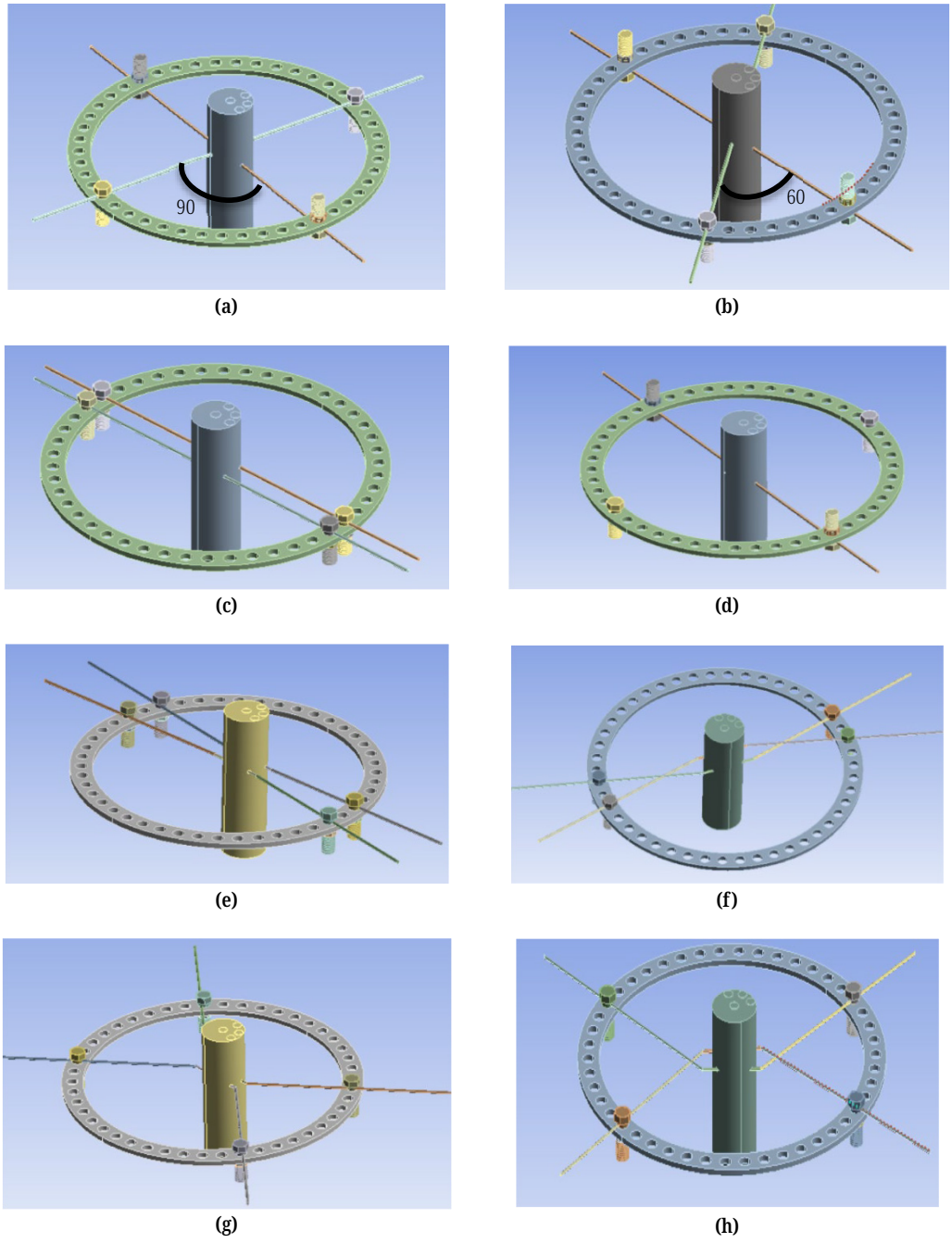

Fig. 5. Wire models (a) stander 90° (b) 60° (c) parallel (d) one wire (e) divergent 1-hole (f) convergent 1-hole (g) divergent 8-hole (h) convergent 8-hole

After that the model was fixed on the rigid iron support and the full model was placed in the testing machine, each model was tested four times (axial compression, medial compression, and posteromedial compression) to 300 N pointed load at 5 mm/s rate using (computer-controlled electronic universal testing machine of max load 100kN) as revealed in Figure 7. For each model and loading case the wires were

replaced with new ones and the procedure was repeated. A load–extension graph was plotted for every test, and displacement data were gathered.

Fig. 6. Wire tensioning by computer-controlled electronic universal testing machine of max load 50KN

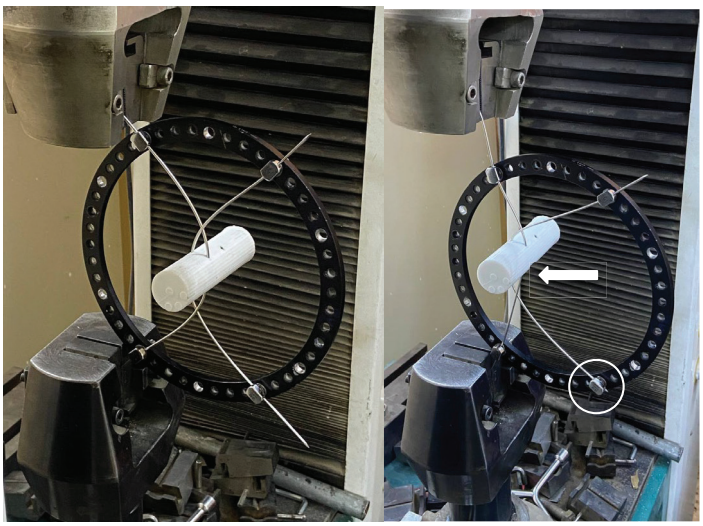

Fig. 7. (Left) the start of tensioning one wire in the convergent 8-hole model, (Right) tensioning causes the cylinder to shift from the center, resulting in slippage of the second wire

2.3 Finite Element Analysis (FEA)

The geometry of the models (ring, bolts, nuts, wires, cylinder) was developed using computer-aided design (CAD) software, SolidWorks, as illustrated in Figure 8.

It is in IGES format and was imported to ANSYS workbench as demonstrated in Figure 9. Material properties of each component were assigned as shown in Table 1.

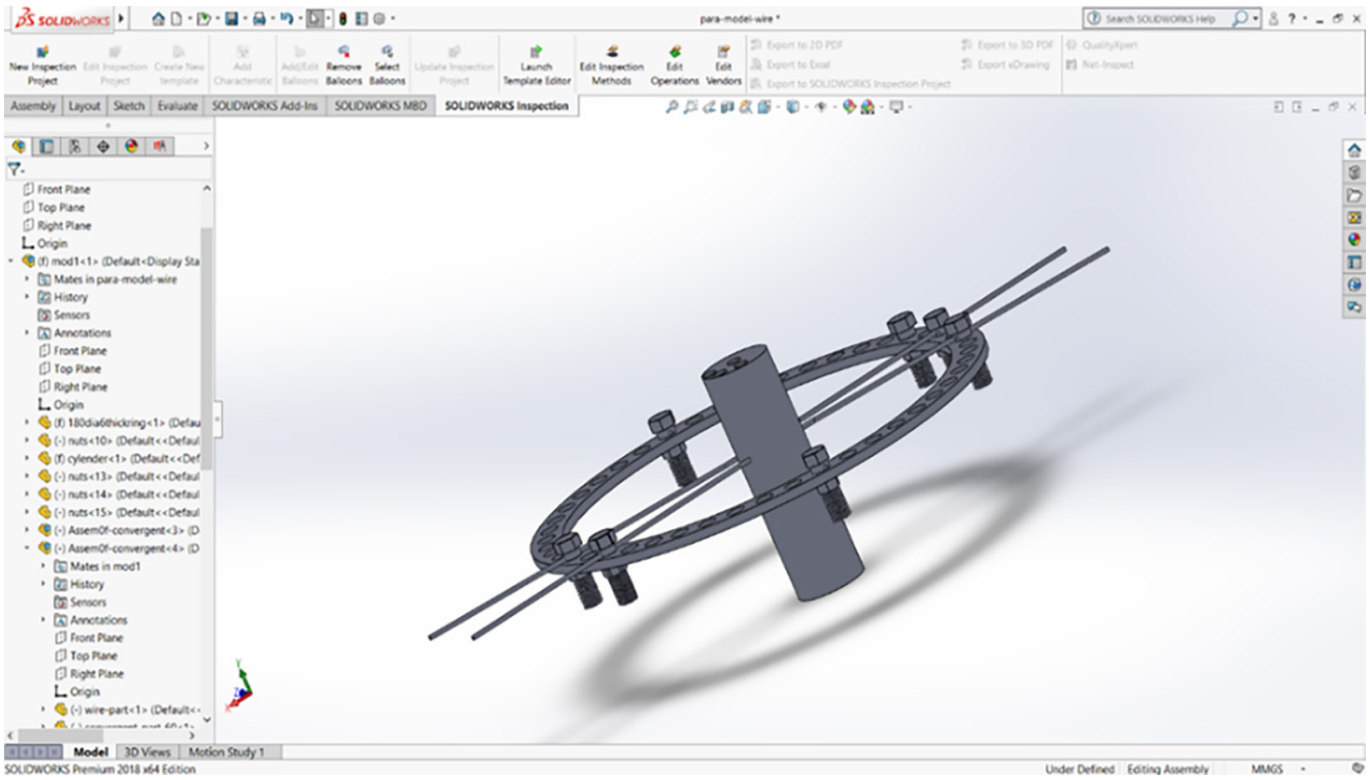

Fig. 8. Models designed by SOLIDWORKS 2018

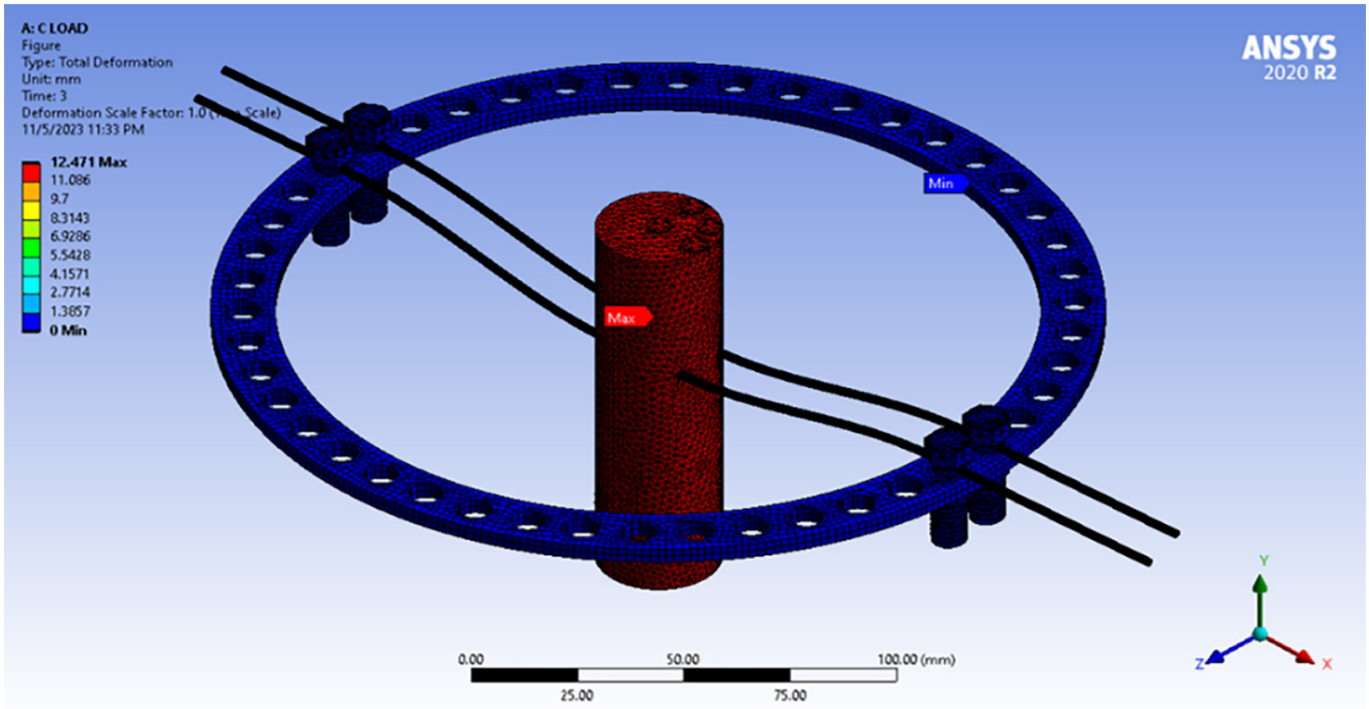

Fig. 9. ANSYS Workbench 2020 R2 was used to conduct Finite Element Analysis (FEA)

Table 1. Properties of the assigned material of the models in ANSYS

Component	Material	Young's Modulus (GPa)	Poisson Ratio
cylinder	PLA	4.107	0.35 [12]
k-wire	316L Stainless steel	210 [13]	0.3 [13]
Bolt, nuts	Stainless steel	193 [14]	0.31 [14]
Ring	Carbon fiber	290	0.2

The density was set to 8 (g/cm^3) for 316 L stainless steel Kirschner wire, and the density for PLA was 1.25 (g/cm^3) [11,15]. To ensure that the bone cannot slide freely along the wire in simulation, all interactions between the wires and the holes in the bone were defined as bonded. The element size of the mesh structure of wires and other components was defined as 0.2 and 2 mm respectively. The number of nodes and elements of each model is shown in Table 2.

Table 2. Number of nodes and elements

Model	Node Number	Element Number
1	2,467,748	622,047
2	2,548,775	682,669
3	2,548,302	682,390
4	1,315,909	347,364
5	2,739,878	681,969
6	2,745,324	687,594
7	2,708,121	677,949
8	2,756,753	690,305

Parameters like aspect ratio, Jacobian, skewness etc. were used to ensure the mesh quality of the model. Table 3 shows these quality parameters along with the acceptable and the averaged values obtained [16].

Table 3. ANSYS mesh quality parameters statistics

Quality Parameter	Ideal Value	Acceptable Value	Value Obtained
Element Quality	1	More than 0 (1 best and 0 worst)	0.75795
Aspect Ratio	1	Less than 5	2.3976
Jacobian ratio	1	More than 0.6	1.3831
Skewness	0	0–0.75	0.20255
Orthogonal Quality	1	More than 0 (1 best and 0 worst)	0.89998

For loading and boundary conditions, a fixed support was applied to one end of the wires and the lower face of the ring as illustrated in Figures 10 and 11. The iron frame was not assigned to the FEA to reduce the calculation time, and it was found that the presence or absence of the frame won't affect the results, since the iron frame purpose is to stablize the model ring in ANSYS, fixed support neglects the need for it. A force of 883 N applied to the other ends of the wires [17], another force applied to the proximal end of the cylinder at specific faces (central, medial, posterior) of 0–300 N. The maximum total deformation result of the bone-wire assembly was

used to make a graph of load-displacement so it can be compared with the mechanical test graph and validate the FEA.

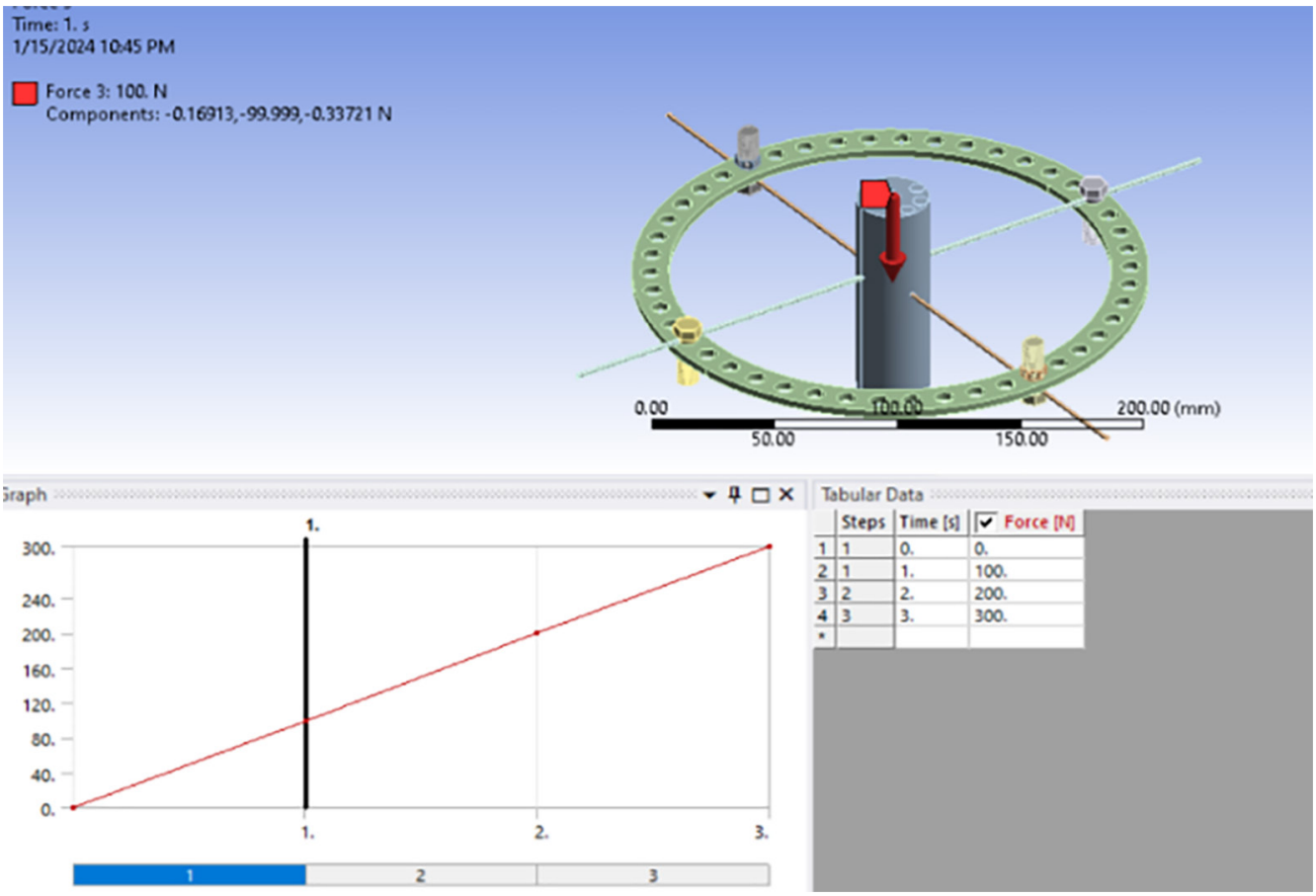

Fig. 10. The loading boundary conditions for central loading condition in the standard wires model

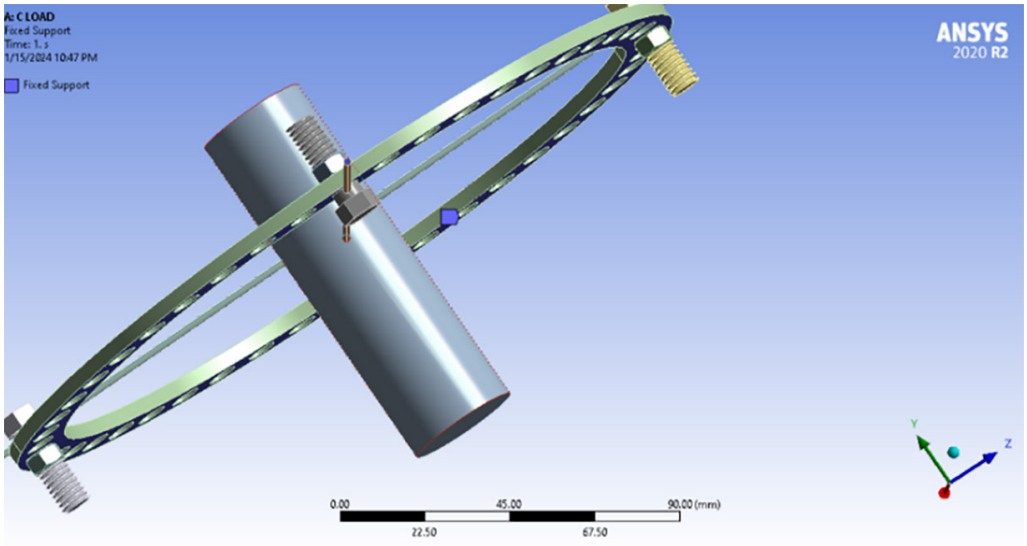

Fig. 11. The fixed support applied on wires and ring in all models that neglect the frame need

More tests can be done on the models like axial torsion of (5 Nm) [18]. When torsion, medial and posterior load are applied, it causes the bending of the cylinder in

the medial-lateral and anterior-posterior axes (represented by X and Z, respectively). The resulting angulations in the X and Z axes can be calculated using FEA.

3 RESULTS AND DISCUSSION

A series of experiments were carried out in order to study the mechanical behavior of the Ilizarov fixator in case of changing wires configuration. After the displacement obtained in central loading in both mechanical and FEA, the stiffness was calculated using the following formula [8].

$$K = F/D \tag{1}$$

Where:
K = stiffness (N/mm) or (N.mm/ deg)
F = force (N) or bending (N.mm)
D = displacement (mm) or angulation (deg)

And for medial bending, posterior bending, and torsion, the angles were calculated using simple trigonometric formulas, and the stiffness then calculated by the same formula (1) by dividing the bending or tension on the angulation obtained [18].

Medial and posterior loading causes 1.2, 2.4, and 3.6 (N.m) for 100, 200, and 300 N loading, respectively. After stiffness was calculated for all loading cases, spss program was used to do the statistics. After the initial loading of the limb, the wire slippage at the bolt wire contact causes the FEA result to show a linear behavior as compared to the mechanical results. Due to significant plastic deformation, bolt/wire slippage results in larger tension loss at the beginning of the loading [19,20].

When modeling wire-bolt contacts ANSYS, they are assigned as bonded contacts, which results in no slippage. Consequently, deflection in wires is caused by plastic deformation resulting in a slightly smaller deflection in FEA.

3.1 Axial compression

Axial compression is the primary loading mechanism for weight-bearing and is the most important mode of loading for an Ilizarov fixator [21].

After analyzing the ANOVA tables for the mechanical and FEA data using spss, it was determined that the difference between the models was statistically significant ($p < 0.001$). After conducting Post Hoc Tests, it was found that all models, except for the one-wire and convergent 8-hole separation models, showed no statistically significant difference with the standard model and the 60-crossing angle model in mechanical aspects. The two models had a p-value less than 0.05, indicating a significant difference. And as shown in Figure 12 the fourth model and last model show higher displacements compared to other models.

In FE aspects, it was found that all models, except for divergent 1-hole separation models, showed statistically significant differences with the standard model and the 60-crossing angle model. Figure 12 displays the mean stiffness of different models. The sixth model, which is the convergent 1-hole separation model, demonstrates the highest axial compression stiffness in both mechanical and FEA.

In the Ilizarov technique, the rigidity under axial loading is not affected by the angles between the wires. However, crossing the wires at smaller angles can cause uneven forces to be applied to the rings, resulting in the deformation of the rings. This can lead to a decrease in axial stiffness in some cases, which is why the standard wire configuration does not have the highest performance [22].

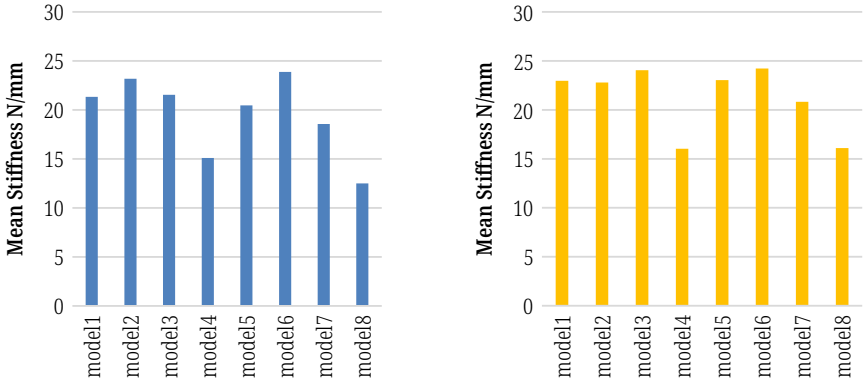

Fig. 12. Stiffness means of models for mechanical result (left) and FEA results (right)

3.2 Medial bending

Statistics show that all models differ significantly from the standard and 60-crossing angle models, with a p-value of less than 0.05 in both X and Z directions. Figure 13 shows the mean stiffness of different models. It can be observed that models 5 and 6 have the highest stiffness in X medial bending. Model 3 has a higher stiffness compared to the standard model. This is because it has two wires in the mediolateral direction, and the wire angle is reduced from 90 degrees. This reduction in wire angle results in increased mediolateral bending stiffness, which explains why the standard model has lower stiffness [22,23].

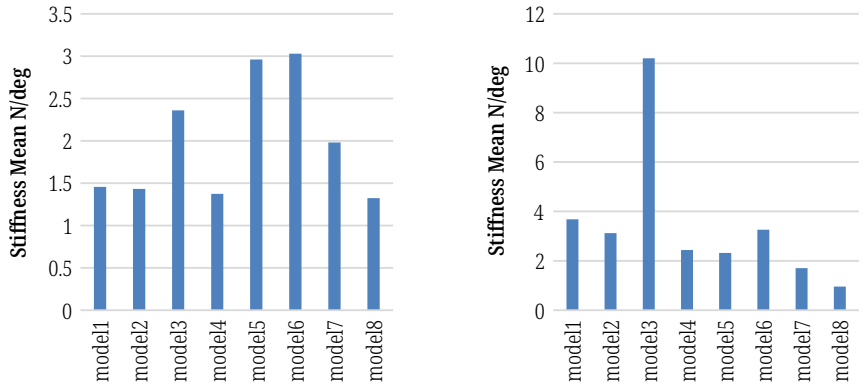

Fig. 13. Stiffness means of models in X (left) and Z medial bending (right)

However, in Z medial bending, stiffness is highest in model 3 (parallel), followed by the standard model. All other models have lower stiffness due to the absence of wire support in the Z direction (anteroposterior). That means the parallel wires stabilize the bone without allowing angulation in other direction under medial bending.

3.3 Posterior bending

According to the statistics, all models are significantly different from the standard and 60-crossing angle models in both X and Z directions, with a p-value of less than 0.05. Figure 14 presents the mean stiffness of various models.

The bending in the Z-direction (posterior) is most significant in the standard model due to the presence of a wire in this direction, resulting in the highest stiffness. Model 2, which has 60 crossing wires, is less stiff due to reduced anteroposterior bending stiffness resulting from the wire angle. Other models without anteroposterior wire have lower rigidity [22,23].

The stability in the X direction during posterior bending is higher in divergent models followed by parallel models.

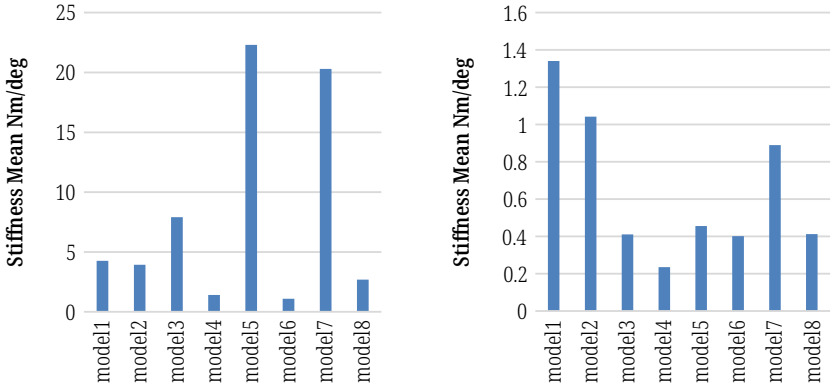

Fig. 14. Stiffness means of models in X (left) and Z (right) posterior bending

3.4 Torsion

Figure 15 shows the mean torsional stiffness for various models. It shows that the parallel model and its improved version have the highest stiffness, while the convergent 8-hole separation model performs the best. Wires crossing at 60 degrees showed significantly greater stiffness in torsion compared to wires crossing at 90 degrees. This is because, similar to axial loading, torsional loading is also independent of the angle between the wires, and when reducing the angle between wires the stiffness increases [22].

When making divergent and convergent models, wires will be bent causing bending movement, which rapidly approaches an asymptotic value, and as the curvature of the wire is increased, the stiffness is increased in the central portion of the beam. The low stiffness at the inner and outer surfaces lessens the maximum stress, while when the beam is homogeneous, the highest stress occurs at the inner and outer surfaces of the beam [24,25].

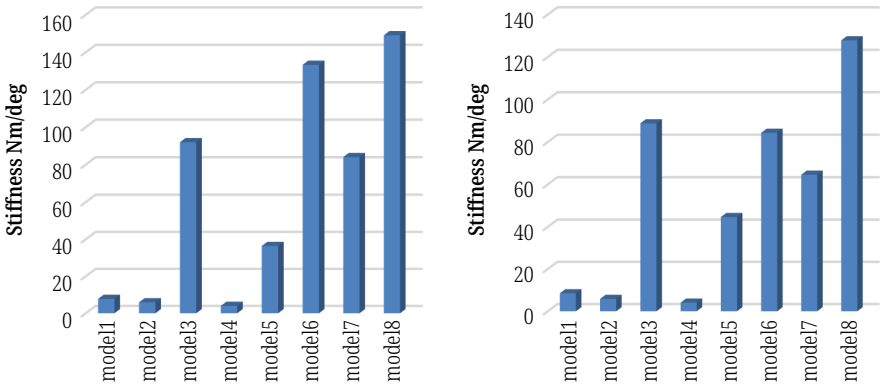

Fig. 15. Torsional stiffness X (left) and Z (right)

When inserting a wire into a bone, if the direction deviates from a straight line perpendicular to the bone, then part of the force that is supposed to push the wire in will be converted into a sideways force. This sideways force is called the tangential component. The more the wire deviates from the perpendicular direction, the greater the tangential component becomes. As a result, increasing the space between holes improves stiffness in divergent models because the tangential component of wires increases. In convergent models, increasing the hole separation decreases the stiffness and increases the tangential components, but the force distribution differs and requires further examination into how it is dispersed and how the tangential components add up or cancel each other [26].

When a curved wire is tensioned, part of that tension is converted into a "cutting force" that leads the wire tract to enlarge leading to loosening. In addition, there will be a contraction in the length of the wire, leading to loss of tension. The wire is only impacted by changes in the hardness parameter (H) once a plastic field starts to form due to bending. The fluctuation of H determines the location and size of the maximum stress in the wire. The maximum stress tends to diminish in magnitude and may move from the inner to the outer surface of bending as H grows in the radial direction. Increasing the hardness will increase the possibility of wire breakage [25,26].

4 CONCLUSIONS

The parallel wire exhibits similar stiffness to standard wire in axial loading and is stiffer in medial bending due to the presence of two wires in the mediolateral plane. However, in the anteroposterior plane, the parallel wire configuration is not as stiff as standard wire and requires stabilization in this direction, where the stiffness of a model represents how the model resists unwanted slide of the bone from its healing position that affects the healing process. Placing a half-pin in this direction will increase the stability and rigidity of the model.

A revised version of the parallel model, known as the divergent models, displays no significant difference in stiffness under axial loading compared to the standard model. However, it exhibits higher medial bending stiffness and a statistcally significant lower stiffness when subjected to posterior bending. Increasing the hole-separation from one to eight boosts rigidity in axial compression, medial bending, and posterior bending, making the 8-hole model ideal for achieving good stiffness in posterior bending. A second revised version of the parallel model, called the convergent model, has the highest stiffness when subjected to axial compression and medial bending. However, it has significantly lower posterior bending compared to the standard model. The convergent model behaves differently from the divergent model, where rigidity decreases as the hole separation increases from one to eight holes. Torsional rigidity is higher in the parallel and modified models, with the most rigidity to torsion found in the convergent and divergent 8-hole separation. It is important to mention that this study does not take into consideration the long-term effects of treatment on the soft tissue surrounding the bone.

5 REFERENCES

[1] G. A. Ilizarov, "Transosseous osteosynthesis: Theoretical and clinical aspects of the regeneration and growth of tissue," Springer Science & Business Media, 2012.

[2] O. Jawad, S. Hamandi, and S. Al-Hussainy, "Effect of the Ilizarov bone fixation on gait cycle and its parameters," 2020. https://doi.org/10.3991/ijoe.v16i11.16155

[3] P. J. Hillard, A. J. Harrison, and R. M. Atkins, "The yielding of tensioned fine wires in the Ilizarov frame," in *Proceedings of the Institution of Mechanical Engineers, Part H: Journal of Engineering in Medicine*, vol. 212, no. 1, pp. 37–47, 1998. https://doi.org/10.1243/0954411981533809

[4] R. Aquarius, A. Van Kampen, and N. Verdonschot, "Rapid pre-tension loss in the Ilizarov external fixator: An in vitro study," *Acta Orthopaedica*, vol. 78, no. 5, pp. 654–660, 2007. https://doi.org/10.1080/17453670710014356

[5] P. Su, S. Wang, Y. Lai, Q. Zhang, and L. Zhang, "Screw analysis, modeling and experiment on the mechanics of tibia orthopedic with the Ilizarov external fixator," *Micromachines*, vol. 13, no. 6, Art. no. 932, 2022. https://doi.org/10.3390/mi13060932

[6] N. Pervan, A. Muminović, E. Mešić, M. Delić, and E. Muratović, "Analysis of mechanical stability for external fixation device in the case of anterior-posterior bending," *Advances in Science and Technology Research Journal*, 2022. https://doi.org/10.12913/22998624/146857

[7] G. L. Orbay, V. H. Frankel, and F. J. Kummer, "The effect of wire configuration on the stability of the Ilizarov external fixator," *Clinical Orthopaedics and Related Research*, vol. 279, pp. 299–302, 1992. https://doi.org/10.1097/00003086-199206000-00038

[8] R. A. Wilkes, A. Harrison, and R. M. Atkins, "Assessment of mechanical stability of a parallel wire bone transport system for use with an Ilizarov frame," in *Proceedings of the Institution of Mechanical Engineers, Part H: Journal of Engineering in Medicine*, vol. 209, no. 3, 1995, pp. 197–202. https://doi.org/10.1243/PIME_PROC_1995_209_343_02

[9] E. Rezabeigi, P. Wood-Adams, and R. Drew, "Production of porous polylactic acid monoliths via nonsolvent induced phase separation," *Polymer*, vol. 55, pp. 6743–6753, 2014. https://doi.org/10.1016/j.polymer.2014.10.063

[10] Y. He, W. Xu, H. Zhang, and J. Qu, "Constructing bone-mimicking high-performance structured poly(lactic acid) by elongational flow field and facile annealing process," *ACS Applied Materials & Interfaces*, 2020. https://doi.org/10.1021/acsami.0c01528

[11] E. Yilmaz *et al.*, "Mechanical performance of hybrid Ilizarov external fixator in comparison with Ilizarov circular external fixator," *Clinical Biomechanics*, vol. 18, no. 6, pp. 518–522, 2003. https://doi.org/10.1016/S0268-0033(03)00073-1

[12] A. Gherissi, R. B. Cheikh, É. Devaux, and F. Abbassi, "Cellulose whiskers micro-fibers effect on the mechanical properties of PP and PLA composites fibers obtained by spinning process," *Applied Mechanics and Materials*, vol. 146, pp. 12–26, 2012. https://doi.org/10.4028/www.scientific.net/AMM.146.12

[13] D. B. Kumar, K. Vijayakumar, A. V. Martin, and R. George, "Review of biomechanical characteristics of Ilizarov ring fixators using FEA," in *IOP Conference Series: Materials Science and Engineering*, IOP Publishing, vol. 993, no. 1, 2020, p. 012037. https://doi.org/10.1088/1757-899X/993/1/012037

[14] G. Zhang, "Geometric and material nonlinearity in tensioned wires of an external fixator," *Clinical Biomechanics*, vol. 19, no. 5, pp. 513–518, 2004. https://doi.org/10.1016/j.clinbiomech.2004.01.009

[15] O. Verim, M. Volkan Yaprakci, and A. Karabulut, "Biomechanical optimization of a novel circular external fixator (optimization of circular external fixator)," *Journal of Medical and Biological Engineering*, vol. 37, pp. 760–768, 2017. https://doi.org/10.1007/s40846-017-0242-4

[16] S. R. Patil, K. P. Powar, and S. M. Sawant, "Thermal analysis of magnetorheological brake for automotive application," *Applied Thermal Engineering*, vol. 98, pp. 238–245, 2016. https://doi.org/10.1016/j.applthermaleng.2015.11.128

[17] T. Toumanidou, L. A. Spyrou, and N. Aravas, "A finite element model of the Ilizarov fixator system," in *2011 10th International Workshop on Biomedical Engineering*, IEEE, 2011, pp. 1–4. https://doi.org/10.1109/IWBE.2011.6079016

[18] V. Antoci, M. J. Voor, V. Antoci Jr, and C. S. Roberts, "Biomechanics of olive wire positioning and tensioning characteristics," *Journal of Pediatric Orthopaedics*, vol. 25, no. 6, pp. 798–803, 2005. https://doi.org/10.1097/01.bpo.0000184646.03981.ec

[19] B. Fleming, D. Paley, T. Kristiansen, and M. Pope, "A biomechanical analysis of the Ilizarov external fixator," *Clinical Orthopaedics and Related Research* (1976–2007), vol. 241, pp. 95–105, 1989. https://doi.org/10.1097/00003086-198904000-00012

[20] V. La Russa, B. Skallerud, J. Klaksvik, and O. A. Foss, "Reduction in wire tension caused by dynamic loading: An experimental Ilizarov frame study," *Journal of Biomechanics*, vol. 44, no. 8, pp. 1454–1458, 2011. https://doi.org/10.1016/j.jbiomech.2011.03.018

[21] K. P. Baidya, S. Ramakrishna, M. Rahman, and A. Ritchie, "Advanced textile composite ring for Ilizarov external fixator system," in *Proceedings of the Institution of Mechanical Engineers, Part H: Journal of Engineering in Medicine*, vol. 215, no. 1, 2001, pp. 11–23. https://doi.org/10.1243/0954411011533490

[22] C. S. Roberts, V. Antoci, V. Antoci Jr, and M. J. Voor, "The effect of transfixion wire crossing angle on the stiffness of fine wire external fixation: A biomechanical study," *Injury*, vol. 36, no. 9, pp. 1107–1112, 2005. https://doi.org/10.1016/j.injury.2004.08.018

[23] D. G. Bronson, M. L. Samchukov, J. G. Birch, R. H. Browne, and R. B. Ashman, "Stability of external circular fixation: A multi-variable biomechanical analysis," *Clinical Biomechanics*, vol. 13, no. 6, pp. 441–448, 1998. https://doi.org/10.1016/S0268-0033(98)00007-2

[24] J. Chakrabarty, W. B. Lee, and K. C. Chan, "An exact solution for the elastic/plastic bending of anisotropic sheet metal under conditions of plane strain," *International Journal of Mechanical Sciences*, vol. 43, no. 8, pp. 1871–1880, 2001. https://doi.org/10.1016/S0020-7403(01)00009-1

[25] J. Dryden, "Bending of inhomogeneous curved bars," *International Journal of Solids and Structures*, vol. 44, nos. 11–12, pp. 4158–4166, 2007. https://doi.org/10.1016/j.ijsolstr.2006.11.021

[26] E. Arslan and A. N. Eraslan, "Bending of graded curved bars at elastic limits and beyond," *International Journal of Solids and Structures*, vol. 50, no. 5, pp. 806–814, 2013. https://doi.org/10.1016/j.ijsolstr.2012.11.016

6 AUTHORS

Alaa A. Najim, B.S. She got her B.Sc. degree in biomedical engineering in 2019 from Al-Nahrain University/College of Engineering, Baghdad, Iraq. and is presently a student of master's in biomedical engineering, Al-Nahrain University/College of Engineering, Baghdad, Iraq (E-mail: st.alaa.a.najm@ced.nahrainuniv.edu.iq).

Sadiq J. Hamandi, Ph.D. is currently an Assistant Professor in Biomedical Engineering Department, College of Engineering, Al-Nahrain University, Iraq. He received his B.Sc. degree in Mechanical Engineering in 1992 from Baghdad University in Baghdad, Iraq. His M.Sc. degree in Mechanical Engineering from Al-Nahrain University/College of Engineering in 1994, and his Ph.D. degree in Mechanical Engineering from Al-Nahrain University/College of Engineering in 2000. His presently research interests include Biomechanics and Biotribology. E-mail: sadiq_hamandi@eng.nahrainuniv.edu.iq. The number of articles in national databases 26. The number of articles in international databases 6.

Ahmed Alzubaidi, Ph.D. is currently an Assistant Professor at College of Medicine, Al-Nahrain University, Baghdad, Iraq, Bachelor of Medicine and General Surgery, College of Medicine/Al-Nahrain University, Baghdad, Iraq 1995, Iraqi Board of Traumatology and Orthopedics 2002 (E-mail: ahmed72sabeeh@yahoo.com).